Structural and Functional Correlates of Hallucinations and Illusions in Parkinson's Disease

Ana Luísa Marques, Natasha Taylor, Daniel Roquet, Steven Beze, Carine Chassain, Bruno Pereira, Claire O'callaghan, Simon Lewis, Franck Durif

Journal of Parkinson's Disease xx (2021) x–xx
DOI 10.3233/JPD-212838
IOS Press

Research Report

Structural and Functional Correlates of Hallucinations and Illusions in Parkinson's Disease

Ana Marques[a,b,*], Natasha L. Taylor[a], Daniel Roquet[c], Steven Beze[b], Carine Chassain[d], Bruno Pereira[e], Claire O'Callaghan[a], Simon J.G. Lewis[a] and Franck Durif[b]
[a]*Forefront Parkinson's Disease Research Clinic, Brain and Mind Center, School of Medical Sciences, University of Sydney, Camperdown, Sydney, Australia*
[b]*Université Clermont Auvergne, IGCNC, Institut Pascal, Clermont-Ferrand University Hospital, Neurology Department, Clermont-Ferrand, France*
[c]*Frontiers, Brain and Mind Center, University of Sydney, Camperdown, Sydney, Australia*
[d]*Université Clermont Auvergne, IGCNC, Institut Pascal, Clermont-Ferrand University Hospital, Neuroradiology Department, Clermont-Ferrand University Hospital, Clermont-Ferrand, France*
[e]*Clermont-Ferrand University Hospital, Biostatistics Department, Clermont-Ferrand, France*

Accepted 17 October 2021

Abstract.
Background: Visual illusions (VI) in Parkinson's disease (PD) are generally considered as an early feature of the psychosis spectrum leading to fully formed visual hallucinations (VH), although this sequential relationship has not been clearly demonstrated.
Objective: We aimed to determine whether there are any overlapping, potentially graded patterns of structural and functional connectivity abnormalities in PD with VI and with VH. Such a finding would argue for a continuum between these entities, whereas distinct imaging features would suggest different neural underpinnings for the phenomena.
Methods: In this case control study, we compared structural and resting state functional MRI brain patterns of PD patients with VH (PD-H, $n = 20$), with VI (PD-I, $n = 19$), and without VH or VI (PD-C, $n = 23$).
Results: 1) PD-H had hypo-connectivity between the ILO and anterior cingulate precuneus and parahippocampal gyrus compared to PD-C and PD-I; 2) In contrast, PD-I had hyper-connectivity between the inferior frontal gyrus and the postcentral gyrus compared to PD-C and PD-H. Moreover, PD-I had higher levels of functional connectivity between the amygdala, hippocampus, insula, and fronto-temporal regions compared to PD-H, together with divergent patterns toward the cingulate. 3) Both PD-I and PD-H had functional hypo-connectivity between the lingual gyrus and the parahippocampal region vs. PD-C, and no significant grey matter volume differences was observed between PD-I and PD-H.
Conclusion: Distinct patterns of functional connectivity characterized VI and VH in PD, suggesting that these two perceptual experiences, while probably linked and driven by at least some similar mechanisms, could reflect differing neural dysfunction.

Keywords: Parkinson's disease, hallucinations, illusions, neuroimaging, visuo-perception

*Correspondence to: Ana Marques, MD, PhD, Neurology Department, Place Henri Dunant, CHRU Gabriel Montpied, 63000 Clermont-Ferrand, France. Tel.: +33473751600; E-mail: ar_marques@chu-clermontferrand.fr.

INTRODUCTION

Visual hallucinations (VH), defined as a perception without existing stimuli, are one of the most frequent non-motor symptoms of Parkinson's disease (PD), and typically present across a spectrum ranging from minor hallucinations to complex hallucinations. In contrast, visual illusions (VI), defined as a false perception of an existing stimulus, are generally considered part of the prodrome towards fully formed visual hallucinations in PD, and are frequently classified as minor hallucinations [1, 2]. However, this sequential relationship has not been clearly demonstrated and longitudinal clinical, imaging and/or pathological studies addressing this specific question are lacking in PD [3, 4].

In other conditions such as schizophrenia, it has been shown that the perception of VI is not related to the strength of VH [5]. Indeed, patients with schizophrenia may even have a reduced susceptibility to visual illusions compared to healthy controls [6]. Thus, whilst one might intuitively regard visuoperceptive phenomena as being symptomatically related, they may arise from discrete and separable neural substrates.

Previously, neuroimaging techniques have been used to investigate structural, functional and metabolic changes in PD patients with and without VH [7–14], either including well-structured or minor VH [7, 10], and have reported alterations in multiple regions related to different functions such as visuospatial processing, attention and memory [7]. Indeed, morphometric studies identified atrophy in lingual gyrus, cingulate, precuneus, superior frontal gyrus and inferior frontal gyrus (SFG and IFG), hippocampus, fusiform gyrus in PD patients with VH [7–10, 15–17]. Functional studies have generally highlighted decreased activity in posterior brain regions (occipital, parietal, temporal) corresponding to visual pathways, and increased activity of frontostriatal circuits during visual stimuli processing, suggesting an aberrant top-down visual processing over the normal bottom-up processing, as one of the factors predisposing to VH in PD [11, 18]. However, these findings have not been consistent across all studies, and no alterations in posterior activation during presentation of visual stimuli have been reported in other studies, but instead a significant reduction in the activation of the anterior cingulate gyrus, inferior, middle and superior frontal gyri [19]. More recently, the role of abnormal connectivity of the default mode network (namely in regions such as middle frontal gyrus, posterior cingulate and precuneus) and dorsal attention network in the pathophysiology of VH in PD has been suggested [12, 20]. However, those studies did not discriminate between VH and VI, which are not differentiated in the majority of studies, which could explain some of the reported discrepancies. Indeed, less work has been focused on VI in PD and very few studies so far have addressed the question of brain changes that could be specifically related to either VI or VH [4, 21–23].

One study has shown that the metabolic pattern observed in PD patients with kinetopsia (illusion of movement) was similar to the one observed in PD patients with VH, whereas the misidentification of objects had a different pattern that only partially overlapped with VH [4]. Recently, our own team demonstrated that PD patients with VH had generalized retinal and brain atrophy compared to those with VI, regardless of the disease duration [22]. This finding is in line with another study reporting decreased age-adjusted global grey matter volume in Parkinsonian patients with VH compared to those with VI [24]. Yet, these observations failed to resolve whether the brain changes underpinning PD-H simply represent progression from more subtle modifications in PD-I or if these phenomena arise from discrete mechanisms.

We hypothesized that the existence of overlapping but graded patterns of structural and functional abnormalities in PD with VI and VH would argue for a continuum between these entities, whereas distinct functional connectivity features would suggest different neural underpinnings for the phenomena. To test this hypothesis, we assessed group-wise local changes of voxel values throughout the entire brain, and we analyzed the resting state functional connectivity associated with VH and VI in PD, focusing on the following regions: lateral occipital cortex (mid-level visual region involved in shape and object identification) [25], lingual gyrus (supplementary visual cortex) [26], and occipital fusiform gyrus (responsible for high-level visual processing, and for memory multisensory integration and perception) [27], amygdala and insula (involved in emotional processing and emotional modulation of perception) [28], hippocampus (involved in encoding and retrieval of memories, conscious observation and anticipation, and mental imagery) [29], precuneus (involved visuo-spatial imagery, self-processing and consciousness) [30], and inferior/middle/superior frontal gyrus (IFG, MFG, SFG) (involved in retrieval of autobiographical memories and reality

monitoring) [31–34]. Those regions were selected as they were previously reported to be impaired in structural and functional MRI studies conducted in PD patients with VH [7].

MATERIALS AND METHODS

Study design and settings

The participants were a subset drawn from our previous study [22], that included eighty four PD patients, either with VI (PD-I; $n = 28$), VH (PD-H; $n = 28$), and without any VI or VH (PD-C; $n = 28$) matched for age and sex, who were recruited from the Parkinson expert center, Neurology Department, Clermont-Ferrand University Hospital, France, between March 2018 and April 2019. Among these patients, 68 underwent MRI (PD-I: $n = 22$, PD-H: $n = 23$, PD-C: $n = 23$) and were included in the current study. We assessed the characteristics of VH and VI, severity of PD, as well as dopaminergic treatment, general cognitive and specific visuo-perceptive functions. Neuroimaging evaluated brain volumetry and functional connectivity for all patients. The protocol was approved by the South-West & Overseas II ethical committee, France (clinicaltrials.gov number NTC03454269). All patients gave their written informed consent as per the Declaration of Helsinki.

Participants

We included PD patients who met the United Kingdom Parkinson's Disease Society Brain Bank criteria [35], and the presence of VI or VH was defined using the scale for outcomes in PD psychiatric complication (SCOPA-PC) [36], together with patient and caregiver interviews. Inclusion criteria required that VI or VH had to occur at least once a week within the past 3 months. VI was defined by the false perception of an existing stimulus [37], while VH was defined as a visual perception in the absence of an external stimulus [24]. We only considered visual misperception as VI and we distinguished them from sense of presence and passage hallucinations. Among 68 PD patients ($n = 23$ PD-C; $n = 22$ PD-I; $n = 3$ PD-H), we excluded from our analysis six patients who reported coexisting VH and VI ($n = 3$ PD-H with mild VI, and $n = 3$ PD-I with mild VH), in order to avoid any confounding effect on the brain structural and functional characteristics related to VI or VH (Supplementary Material Flow Diagram). We excluded patients with neurological diseases other than PD or psychiatric conditions characterized by VH, patients with cognitive impairment (Montreal Cognitive Assessment (MoCA) [38] score < 21/30) or with conditions incompatible with MRI scanning (e.g., claustrophobic, severe camptocormia, weight restrictions, congestive cardiac failure, severe dyskinesia or tremor). Treatment with antipsychotics represented a further exclusion, as well as modifications of anti-parkinsonian treatments within the month before inclusion.

Clinical and neuropsychological assessments

The characteristics and severity of visual hallucinations or illusions were assessed according to the Psycho-Sensory hAllucinations Scale (PSAS) [39]. The presence of other modalities such as sense of presence, passage hallucinations, auditory, olfactory and cenesthesis hallucinations was also noted. We assessed the duration and severity of PD (according to Movement Disorder Society - Unified Parkinson's Disease Rating Scale (MDS-UPDRS) [40] and Hoehn & Yahr stage [41], and noted the dopaminergic treatment doses (expressed as total Levodopa equivalent dose (LED)) [42], as well as other treatments users (antidepressants, benzodiazepine, cholinesterase inhibitors, antiepileptics).

Cognitive profile (including Mattis dementia rating scale [43], and the copy of the complex figure of Rey-Osterrieth [44]), sleep quality (Parkinson's disease sleep scale (PDSS-2) [45], probable REM Sleep Behavior Disorder (screened with REM Sleep Behavior Disorder Single-Question (RBD-1Q) [46], and excessive daytime sleepiness (Epworth scale) [47] were assessed. Subjective ophthalmological complaints (vision loss, visual field impairment, metamorphopsia, halos, diplopia, color vision complaint, epiphora, eye pains) were noted during a semi structured interview with an ophthalmologist. All clinical and neuropsychological assessments, as well as neuroimaging, were performed with participants on their regular antiparkinsonian treatment.

Imaging acquisition and analysis

Acquisition

MRI scans were performed at 3T on a General Electric (3T Discovery MR 750, GE Medical Systems, Milwaukee, Wis; 32 Ch head coil, gradients: 40/200, software: DV24R02) ($n = 44$ patients; 17 PD-C, 15 PD-H, 12 PD-I) and a Siemens scanner (3T Magnetom Vida, Siemens Healthcare, Erlangen, Germany; 64 Ch head coil, hypergradients XT gradients:

Table 1
Demographical, clinical, and neuropsychological characteristics of parkinsonian patients with visual illusions, with visual hallucinations and controls

	PD-C ($n = 23$)	PD-I ($n = 19$)	PD-H ($n = 20$)	p
Age (y)	69.21 ± 8.76	68.31 ± 6.8	70.2 ± 7.35	0.54
Sex (M/F)	14/9	10/9	12/8	0.85
Education level (y)	17.72 ± 3.28	17.9 ± 3.71	18.95 ± 3.81	0.75
Disease duration (y)	6.21 ± 5.06	9 ± 5.33	11.15 ± 6	**0.004**[b]
Hoehn and Yahr (score 0–21)	2.32 ± 1.00	2.5 ± 0.81	2.9 ± 0.88	0.15
MDS-UPDRS Total (score 0–260)	49.91 ± 31.01	55.94 ± 24.74	75.9 ± 31.6	**0.01**[b]
MDS-UPDRS I (score 0–52)	8.47 ± 4.96	13.26 ± 6.02	18.25 ± 6.07	**< 0.001**[a,b,c]
MDS-UPDRS II (score 0–52)	10.73 ± 8.93	13.26 ± 5.09	17.8 ± 9.1	**0.01**[b]
MDS-IPDRS III (score 0–132)	28.69 ± 18.07	27.89 ± 14.30	33.9 ± 18.48	0.43
MDS-UPDRS IV (score 0–24)	2 ± 2.77	2.94 ± 3.23	5.95 ± 5.26	**0.03**[b]
SCOPA-PC (score 0–21)	0.30 ± 0.55	3.45 ± 1.87	4.78 ± 3.10	**< 0.001**[a,b]
PDSS (score 0–60)	10.78 ± 6.66	13.83 ± 6.34	13.65 ± 5.81	0.20
Epworth (score 0–24)	6.86 ± 4.51	8.63 ± 6.09	8.3 ± 5.62	0.55
RBD (%)	6 (26%)	8 (42%)	14 (70%)	**0.01**[b]
Ophthalmological complaints	9 (23%)	11 (57%)	6 (30%)	0.19
PSAS (score 0–23)	0	8.63 ± 2.61	10.3 ± 3.77	**< 0.001**[a,b]
Auditory hallucinations (%)	0 (0%)	0 (0%)	3 (15%)	0.056
Olfactory hallucinations (%)	0 (0%)	0 (0%)	5 (25%)	**0.004**[b]
Cenesthesic hallucinations (%)	0 (0%)	0 (0%)	1 (5%)	0.62
Passage hallucinations (%)	0 (0%)	0 (0%)	2 (10%)	0.11
Presence sensation (%)	1 (4%)	3 (15%)	2 (10%)	0.45
LED total (mg/day)	953.49 ± 521.44	1061.36 ± 439.69	1012.79 ± 627.29	0.68
LED DA (mg/day)	143.46 ± 173.41	212.45 ± 230.09	266.17 ± 634.88	0.35
DA users (%)	15 (65%)	15 (78%)	11 (55%)	0.28
Rivastigmine users (%)	1 (4%)	0 (0%)	2 (10%)	0.50
Antiepileptic users (%)	2 (8%)	5 (26%)	3 (15%)	0.38
Antidepressant users (%)	1 (4%)	10 (52%)	8 (40%)	**0.001**[a,b]
Benzodiazepine users (%)	0 (0%)	7 (36%)	6 (30%)	**0.002**[a,b]
Opioid users (%)	0 (0%)	1 (5%)	0 (0%)	0.29
MoCA	25.88 ± 2.52	26.4 ± 2.74	25.53 ± 2.36	0.66
Mattis				
Total (score 0 to 144)	132.78 ± 9.98	132.78 ± 9.14	127.45 ± 9.14	**0.04**
Attention (score 0 to 37)	36.08 ± 0.90	35.61 ± 0.97	35.4 ± 1.81	0.36
Initiation (score 0 to 37)	32.65 ± 4.68	30.72 ± 4.46	29 ± 5.06	**0.03**[b]
Construction (score 0 to 6)	5.69 ± 0.63	5.55 ± 0.61	5.7 ± 0.47	0.57
Conception (score 0 to 39)	36.26 ± 3.95	36.66 ± 2.95	36.4 ± 3.40	0.94
Memory (score 0 to 25)	22.08 ± 2.52	21.94 ± 2.41	20.95 ± 2.66	0.33
Rey-complex figure (score 0 to 36)	28.2 ± 10.4	27.5 ± 10.25	24.52 ± 10.18	0.20

Mattis, Mattis Dementia Rating Scale; MoCA, Montreal Cognitive Assessment (Score 0 to 30); PD-C, control patients with Parkinson's disease; PD-H, patients with Parkinson's disease and visual hallucinations; PD-I, patients with Parkinson's disease and visual illusions; PDSS, Parkinson Disease Sleep Scale; PSAS, Psychosensory Hallucinations Scale; RBD, REM sleep behavior disorder; SCOPA-PC, scale for outcomes in Parkinson's disease-psychiatric complication; Results are expressed as means ± standard deviation, and number of patients (%). The comparisons between 3 groups were performed using chi-squared or Fisher's exact tests for categorical variables and the analysis of variance (ANOVA) or Kruskal-Wallis test for quantitative parameters. When appropriate (omnibus p-value less than 0.05), a *post-hoc* test was applied for multiple comparisons ([a]$p < 0.05$ between PD-I and PD-C; [b]$p < 0.05$ between PD-H and PD-C; [c]$p < 0.05$ between PD-I and PD-H).

60/200, software: XVA 11-A) ($n = 24$ patients; 6 PD-C, 8 PD-H, 10 PD-I), due to change of scanner at our site during the study. The precise technical characteristics of each sequence have been harmonized between the two scanners in order to achieve the most homogeneous imaging data possible. A particular effort has been made on the definition of TR, TE, flip angle (α), bandwidth, acceleration, temporal and spatial resolution, and field of view. This step was carried out using a NIST test object associated with a quality control procedure to quantify various geometric and signal parameters [48]. MRI scanners, scans protocol and parameters were qualified after images quality analysis by the CATI platform (Centre d'Acquisition et de Traitement d'Images, Multicenter Neuroimaging Platform, Paris, France) to confirm the acquisition reproducibility. Acquisition parameters are detailed in the Supplementary Material.

Volumetric brain analysis

Pre-processing (Supplementary Material) and analysis were performed using Statistical Parametric Mapping software (SPM12, Welcome Trust Centre for neuroimaging, London, UK, http://www.fil.ion.ucl.ac.uk/spm/) implemented in Matlab 2018a. A voxel-wise one-way ANOVA was performed to compare grey matter intensity across groups, with PD duration (years since symptoms onset), scanner manufacturer (Siemens or GE) and total intracranial volume as regressors of non-interest. Age and sex were not included as covariates since groups were matched for these variables. Statistical analysis combined a p uncorrected <0.001 threshold at the voxel level and an extent threshold of 100 adjacent voxels. Clusters which survived a multiple comparison correction (Family Wise Error rate) $p_{FWE}<0.05$ at the cluster level were explicitly labelled in the tables. Neuroanatomical regions of significance were visualized and identified using xjview toolbox (https://www.alivelearn.net/xjview).

Resting state fMRI analysis

Preprocessing (Supplementary Material) and seed-based connectivity analysis were performed using Conn functional connectivity toolbox (19.b) (http://www.nitrc.org/projects/conn, RRID:SCR_009550) [49], which streamlines functions from SPM12. A seed-based connectivity analysis calculates the functional connectivity between a selected region of interest (ROI), the seed, with all the voxels in the brain. The analysis estimates the Fisher-transformed bivariate correlation coefficient between the seed BOLD signal and all the voxels BOLD signal across time. The following ROIs were selected (FSL Harvard-Oxford cortical/subcortical atlas, maximum probability threshold 25%, 1 mm, https://identifiers.org/neurovault.collection:262): putamen, caudate, lateral occipital cortex, lingual gyrus and occipital fusiform gyrus, amygdala and insula, hippocampus, precuneus and inferior/middle/superior frontal gyrus (IFG, MFG, SFG) [31–34].

Then, we compared seed-to-voxel connectivity maps across participant groups using a generalized linear model to perform multivariate regressions looking at contrasts between participant groups and controlling for age, duration of disease, benzodiazepine and antidepressant treatments and MRI scanner type. We performed parametric statistical testing, for comparisons between the three groups using two-sample *t*-tests for between two group differences and one-way ANOVA. We calculated the uncorrected *p*-value and false-discovery rate, with statistical significance specified at $p<0.05$.

Statistical analysis of clinical data

Statistical analyses were performed using Stata software version 15 (StataCorp, College Station, US). For continuous data, the assumption of normality was assessed with the Shapiro-Wilk test. The comparison between groups for categorical data were performed using Chi-squared test and when appropriate Fisher's exact test, whereas the comparisons for continuous variables were carried out using ANOVA and Kruskal-Wallis test when assumptions required for ANOVA were not met. The homoscedasticity was analyzed using the Bartlett test. When appropriate (omnibus *p*-value <0.05), *post-hoc* tests for two by to multiple comparisons were applied, respectively Tukey-Kramer after ANOVA, Dunn's test after Kruskal-Wallis and Marascuilo procedure after Chi-squared and Fisher exact tests. All statistical tests were two-sided and a *p*-value <0.05 was considered statistically significant.

RESULTS

Clinical characteristics

Sixty-two PD patients were analyzed for clinical and brain volumetric data ($n=23$ PD-C, $n=19$ PD-I, $n=20$ PD-H), and 58 patients analyzed for resting state functional data ($n=21$ PD-C, $n=19$ PD-I, $n=18$ PD-H) after exclusion of corrupted files (Supplementary Material Flow Diagram). Demographic and clinical characteristics of patients together with group effects are shown in Supplementary Table 1).

MRI analyses

Volumetry

Whole-brain voxel-based morphometry analyses revealed no grey matter volume difference between PD-I and PD-H or between PD-I and PD-C groups. Decreased volume was observed in PD-H versus PD-C in the bilateral supramarginal, middle and superior temporal gyrus, and middle occipital gyrus ($p<0.001$ uncorrected) but did not survive the multiple comparisons correction ($p_{FWE}<0.05$) (Supplementary Table 1 and Supplementary Figure 1).

Seed-based functional connectivity at rest

Overlapping features between PD-I and PD-H. PD-I and PD-H both had functional hypoconnectivity between left lingual gyrus and left

Table 2
Seed-based functional connectivity in parkinsonian patients with visual hallucinations, with illusions and controls

		P_{FDR}-CORR	K_E	*P* UNCORR	BETA	T	X (MM)	Y (MM)	Z (MM)	
PD-I > PD-H										
R AMYGDALA	< 0.001	< 0.001	408	< 0.001	0.19	6.54	66	–38	–02	R MTG
	0.003	0.003	268	< 0.001	0.19	5.05	8	70	–6	R Frontal pole
	0.01	0.006	223	< 0.001	0.18	5.08	–58	24	20	L IFG
L AMYGDALA	0.01	0.02	205	< 0.001	0.20	5.45	–58	12	24	L IFG
R HIPPOCAMPUS	< 0.001	< 0.001	615	< 0.001	0.19	5.38	–60	8	18	L IFG (triang.)
	0.001	0.001	394	< 0.001	0.17	5.28	–14	20	14	L caudate
L INSULA	0.001	0.002	358	< 0.001	0.19	5.07	26	–44	–14	R temporal occipital fusiform cortex
R SFG	< 0.001	< 0.001	518	< 0.001	0.34	5.29	52	18	22	R IFG
L IFG (TRIANG.)	0.01	0.02	239	< 0.001	0.18	5.25	–66	–6	18	L post central gyrus
	0.08	0.04	145	0.005	0.12	4.53	14	–46	–4	R lingual gyrus
	0.05	0.03	165	0.03	0.19	5.36	24	–28	–4	R hippocampus
L CAUDATE	0.01	0.03	215	0.001	0.16	5.30	68	–34	–10	R MTG
PD-I > PD-C										
R SFG	< 0.001	< 0.001	475	< 0.001	–0.08	4.23	–2	–54	30	Posterior cingulate gyrus, precuneus
	0.05	0.04	184	0.003	+0.20	5.57	+12	–22	+42	Posterior cingulate gyrus, r precentral gyrus
R LINGUAL GYRUS	0.10	0.04	135	0.006	– 0.11	5.65	–40	+4	–38	L temporal pole, L temporal fusiform gyrus
L LINGUAL GYRUS	0.06	0.03	160	0.003	–0.07	–5.64	–36	–16	–30	L parahippocampal gyrus, temporal fusiform gyrus
L IFG (TRIANG)	0.03	0.03	181	0.002	0.12	5.35	–66	–10	34	L postcentral gyrus
PD-H > PD-C										
L INFERIOR LATERAL OCCIPITAL CORTEX	0.009	0.01	258	< 0.001	–0.13	5.05	–16	38	10	Anterior cingulate gyrus, L paracingulate
R LINGUAL	0.01	0.01	245	< 0.001	–0.14	5.55	36	2	–44	R parahippocampal gyrus, R temporal fusiform gyrus
	0.005	0.01	281	< 0.001	–0.16	6.58	–42	4	36	L parahippocampal gyrus, L temporal fusiform gyrus
L LINGUAL	< 0.001	< 0.001	462	< 0.001	–0.17	5.85	–40	–4	2	L insular cortex
	0.01	0.009	250	< 0.001	–0.22	5.97	–30	–8	–42	L temporal fusiform gyrus
	0.006	0.004	268	< 0.001	–0.20	5.30	36	6	–46	R temporal fusiform gyrus

IFG, inferior frontal gyrus; ITG, inferior temporal gyrus; K_E, cluster size; L, left; PD-C, Parkinson's disease without illusions or hallucinations; MTG, middle temporal gyrus; PD-H, Parkinson's disease with visual hallucinations; PD-I, Parkinson's disease with visual illusions; pFDR, *p* corrected for multiple comparisons using the false discovery rate; pFWE, *p* corrected for multiple comparisons using the family wise error; puncorr, p uncorrected; R, right; SFG, superior frontal gyrus; STG, superior temporal gyrus; Triang, triangularis; Beta values, represent Fisher-transformed correlation coefficient values: for the PD-I > PD-H contrast, positive beta values suggest a stronger connectivity between the seed and these regions in PD-I compared to PD-H, while negative beta values suggest a lower connectivity between the seed and these regions in PD-I compared to PD-H; for the PD-I > PD-C contrast, positive beta values suggest a stronger connectivity between the seed and these regions in PD-I compared to PD-C, while negative beta values suggest a lower connectivity between the seed and these regions in PD-I compared to PD-C; for the PD-H > PD-C contrast, positive beta values suggest a stronger connectivity between the seed and these regions in PD-H compared to PD-C, while negative beta values suggest a lower connectivity between the seed and these regions in PD-H compared to PD-C; T values, represent the size of the difference relative to the variation in the sample data; x, y, z (mm), coordinates in MNI space. Age, disease duration, MRI manufacturer, and the presence of benzodiazepine and antidepressant treatment were included as covariates.

parahippocampal region compared to PD-C, with no difference between PD-I and PD-H (Table 2, Fig. 1).

Distinct features between PD-I and PD-H. PD-I had hyper-connectivity compared to PD-H between bilateral amygdala and bilateral IFG, between right hippocampus and left IFG and caudate, and between left insula and right temporal occipital fusiform cortex. PD-I also had hyper-connectivity between right SFG and right IFG compared to PD-H (Table 2, Fig. 1). PD-I had functional hyper-connectivity between left IFG and left postcentral gyrus both compared to PD-H and PD-C.

PD-I had hyper-connectivity between SFG and IFG compared to PD-H. Moreover, we observed in PD-I hypo-connectivity between SFG and posterior cingulate compared to PD-C, whereas PD-H had

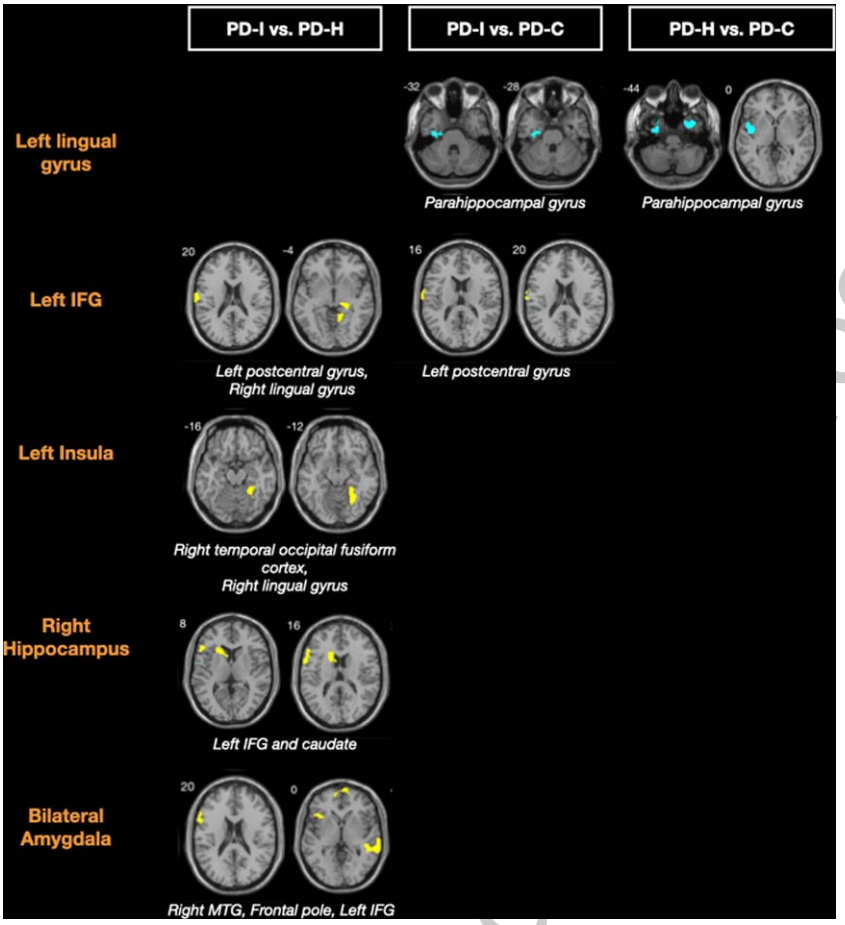

Fig. 1. Seed-based resting state functional connectivity in PD-I, PD-H, and PD-C. For each seed (orange text), differences of functional connectivity between groups are represented; yellow clusters are regions presenting hyper-connectivity with the seed and blue clusters are regions presenting hypo-connectivity with the seed. PD-I and PD-H present a common functional hypo-connectivity pattern between lingual gyrus and parahippocampal region compared to PD-C. Yet, distinct functional patterns are also revealed between VH and VI in PD. PD-I have hyper-connectivity between inferior frontal gyrus (IFG) and postcentral gyrus compared to PD-C and PD-H, and hyper-connectivity between insula and occipital fusiform cortex, and from amygdala, hippocampus towards IFG, compared to PD-H. PD-I, Parkinson's disease patients with visual illusions; PD-H, Parkinson's disease patients with visual hallucinations; PD-C, Parkinson's disease patients without visual hallucinations or illusions.

functional hyper-connectivity between ILO and anterior cingulate and paracingulate.

No other between group differences were reported for other seeds.

Average effect size for each group within clusters with significant between group differences of seed-to-voxel connectivity is represented in Fig. 2.

DISCUSSION

In this study, we compared the volumetric and seed-based functional connectivity characteristics respectively associated with VH and VI in PD. We found no significant structural differences between PD-I and PD-H. However, PD-I and PD-H showed distinct connectivity patterns, although partially overlapping; suggesting that whilst these symptoms share some partly common neural mechanisms, they are also underpinned by specific functional brain differences.

Volumetric characteristics associated with VH and VI in PD

Using voxel-based morphometry (VBM), we observed no volumetric difference between PD-I and PD-H, nor between PD-I compared to PD-C, but found grey matter atrophy in PD-H compared to

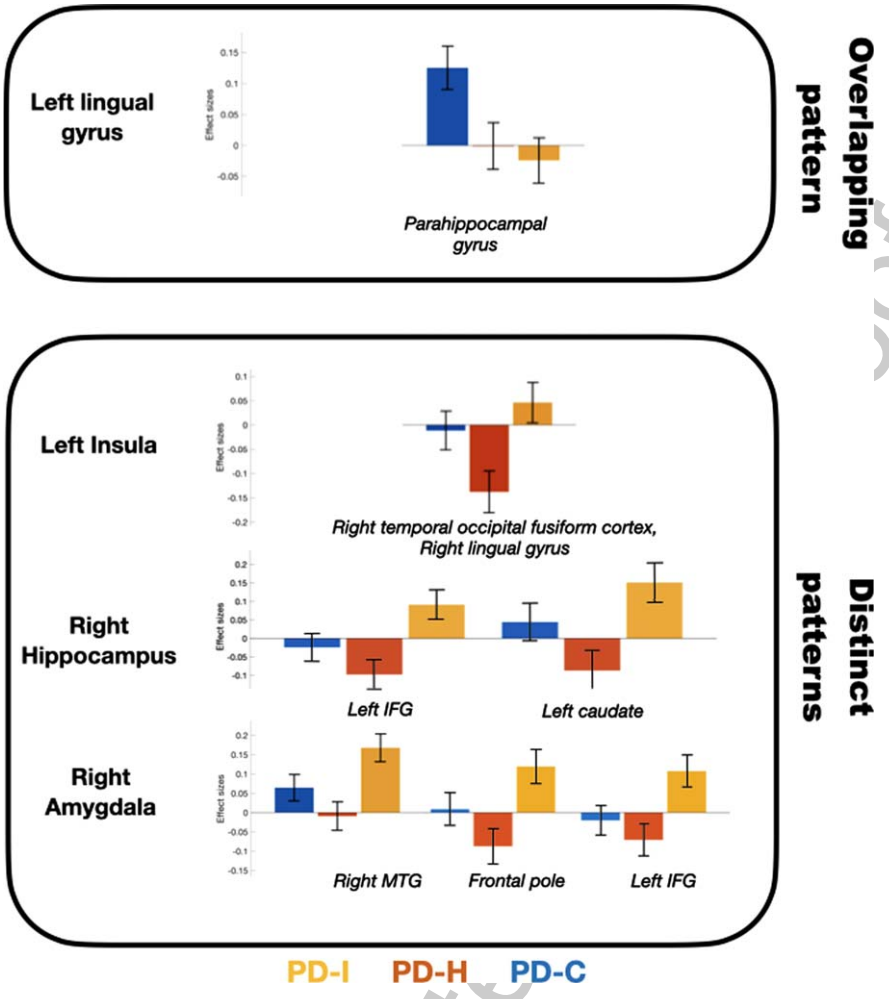

Fig. 2. Average effect sizes in each group within clusters with significant seed-to-voxel differences between PD-I and PD-H. PD-I and PD-H present a common functional hypo-connectivity pattern between lingual gyrus and parahippocampal region compared to PD-. Yet, distinct functional patterns are also revealed between VH and VI in Parkinson's disease. PD-I have hyper-connectivity between insula and occipital fusiform cortex, and from amygdala and hippocampus to IFG compared to PD-H. PD-I, Parkinson's disease patients with visual illusions; PD-H, Parkinson's disease patients with visual hallucinations; PD-C, Parkinson's disease patients without visual hallucinations or illusions.

PD-C in the middle occipital gyrus, and parieto-temporal gyrus, including supramarginal gyrus (uncorrected statistical threshold), indicating a greater degree of neurodegeneration in PD-H. Several other VBM studies have assessed volumetric characteristics associated with VH in PD, and to date, all [8–10, 50–52] but one [17] have reported grey matter volume differences between PD-H and PD-C, in brain regions involved in visuospatial-perception, attention control and memory [7], either using an uncorrected statistical threshold [7, 8, 52], or with correction for multiple comparisons [9, 10, 50, 51]. Structural differences between parkinsonian patients with minor VH (defined by the authors as sense of presence, passage hallucination or illusions) and those with well-structured VH were previously investigated [4], suggesting partly distinct features between complex VH and other manifestations described as minor VH. However, in that study, visual illusions were not distinguished from minor VH. Thus far, only two studies have specifically investigated the morphometric characteristics of PD-I compared to PD-H [22, 24], and reported a decrease in total gray matter volume [22, 24] and left accumbens [22] on brain MRI associated with the presence of VH compared to the presence of VI in PD, independent of age [24], or disease duration [22]. In those studies, including one conducted by our group on the same population, a different tool was used to perform whole brain structural analyses (FreeSurfer), which could explain the

apparently conflicting results compared to the current study [53, 54]. Indeed, in the current study we performed VBM (which utilizes group-wise comparisons that objectively localize focal changes in voxel values throughout the entire brain volume), whereas Freesurfer enables automatic parcellation of the brain into multiple anatomic regions and quantifies tissue volume in these predefined regions on an individual case basis. Thus, even if more widespread brain atrophy has been suggested in PD-H compared to PD-I [22], as of yet, no data suggests the existence of distinct structural changes associated respectively with VH and VI. Hereby, we are currently unable to distinguish between VH and VI according to morphometric characteristics.

Functional connectivity signatures of VH and VI in PD

While we found no VBM difference between PD-I and PD-H in this study, we identified partly overlapping and distinct resting state functional connectivity patterns associated with the presence of VH and VI in PD, independent of disease duration. These connectivity changes observed in PD-H and PD-I could reflect differential deposits of alpha-synuclein, as it has been reported that patients with synucleinopathies frequently experience hallucinations and illusionary perceptions, related to dysfunction of both associative visual areas and changes of limbic areas or the ventral striatum [55].

Common functional connectivity patterns to PD-I and PD-H from lingual gyrus

Both PD-I and PD-H presented functional hypo-connectivity between the lingual gyrus and the parahippocampal region, in line with occipital functional hypo-connectivity generally reported in PD with VH [7, 11, 56]. Hippocampal functional connectivity with the visual cortices has been previously reported to be lower in parkinsonian patients with VH [57], and as suggested by the authors, this could disrupt visuospatial memory and constitute a common functional impairment to VH and VI in PD.

Contrasting functional patterns in PD-I compared to PD-H: hyper-connectivity from IFG, amygdala, hippocampus, and insula

Some contrasting functional differences were revealed between PD-I and PD-H. PD-I compared to PD-H and PD-C had hyper-connectivity between the inferior frontal gyrus (involved in retrieval of episodic memories) [31] and postcentral gyrus. PD-I also had increased connectivity compared to PD-H from the amygdala and hippocampus to the IFG, and from the insula to the occipital fusiform cortex, as well as between SFG and IFG.

Hyper-connectivity between IFG and amygdala, encoding positive and negative emotional memories [58, 59], suggests that emotional memory could influence and modify reality monitoring of an existing visual stimulus in PD with VI. Supporting this hypothesis, pronounced functional connectivity between the amygdala, hippocampus, and right IFG has been reported during autobiographical retrieval in the healthy population [31, 60]. Our findings suggest that VI in PD could be associated with a strong influence of anxiety and fears, and prior experiences on interpretation of visual stimuli, as well as hyperacute reality monitoring, consistently with hyper-connectivity between the insula (involved in the detection of salient stimuli) [61] and the occipital cortex.

Contrasting functional connectivity towards cingulate regions in PD-I and PD-H

Divergent patterns of connectivity between towards the cingulate were also observed in PD-I to PD-C: PD-H had hyper-connectivity from ILO with the anterior cingulate and the anterior paracingulate region compared to PD-C, whilst PD-I had hypo-connectivity from SFG with the posterior cingulate compared to PD-C.

The cingulate cortex has a crucial role in the emergence of VH in PD [62], and it was recently reported that access to consciousness in PD with VH was associated with hypoactivation in the cingulate, suggesting impaired involvement of attentional processing [63]. In particular, the anterior cingulate has a role in focusing attention on behaviorally relevant stimuli [64], whereas the posterior cingulate cortex has a central role in supporting internally-directed cognition, such as autobiographical memories retrieval and conscious awareness [65], and could be differentially involved in VI and VH.

The lateral occipital cortex is a well-known processing center for object recognition [66], and has been reported to activate in fMRI studies in response to pictures of objects, independently of image feature or familiarity [67]. Interestingly, previous neuroimaging studies using regional cerebral

blood flow concluded that the inferior lateral temporal cortex (particularly fusiform gyrus), was the region most likely responsible for the complex visual hallucinations reported in Charles Bonnet Syndrome [68]. As proposed by the authors, visual loss due to eye pathology in Charles Bonnet Syndrome patients, produces a state of sensory deprivation that releases the visual cortex from regulation by external stimuli that normally has an inhibitory effect on the endogenous activation of the visual cortex. Such a cortical release phenomenon could also occur in PD-H patients secondary to retinal impairment [22], and result in visual hallucinations. Furthermore, reduced activity of the superior frontal gyrus has been demonstrated in healthy individuals who are prone to psychosis [33], and in patients with schizophrenia [69]. Contrasting connectivity between cingulate, SFG and ILO could represent distinct neural mechanisms leading to VH or to VI in PD.

Visual and non-visual hallucinations

A significant proportion of PD patients with visual hallucinations also had olfactory hallucinations, and one might argue that it may have play a role in the specific pattern of functional alterations observed in the PD-H group. Yet, olfactory, tactile and gustatory hallucinations usually coexist with VH in PD [70] and in other conditions such as schizophrenia [71, 72], and probably involve the alteration of common pathways responsible for reality monitoring. Indeed, a previous longitudinal study showed that whilst visual hallucinations in isolation are classic in early PD, nonvisual hallucinations emerge over time, and the combination of visual with nonvisual hallucinations predominates in later stages of PD [73]. Moreover, the presence of visual/auditory hallucinations and sex has been reported recently to be the main variables predicting the presence of olfactory hallucinations [74], without any association with olfactory impairment [74, 75]. Thus, hallucinations in PD may occur in one or multiple sensory modalities, and a common brain network responsible for hallucinations independent of the sensory modality has been suggested by previous studies [76]. In line with this hypothesis, a previous study compared PD patients with one versus multiple hallucinatory modalities, and did not reveal any difference regarding demographic, clinical and medication parameters [72]. Interestingly, we found that other sensory modalities of hallucinations are only reported in PD patients with visual hallucinations and not in PD patients with illusions, thus appearing to be part of a common clinical spectrum related to the functional alterations reported in our results.

Limitations

Our study has several limitations that should be considered when interpreting the results. First, our study is ancillary, and analyses were conducted in a sample whose size was calculated for a previous analysis focusing on retinal thickness. Thus, the sample size may have been too small to identify VBM differences between PD-I and PD-C. However, 62 parkinsonian patients were included in our functional data analysis, which is higher than the majority of previous functional neuroimaging studies on parkinsonian patients with VH [7]. Another limitation of this study is the difficulty to distinguish VI from minor hallucinations such as passage hallucinations and sensation of presence. Presence hallucinations could be identified, during patients and caregiver interview, as they are closer to a delusional idea or a social hallucination and defined by the belief that a person is present behind oneself generally, but without associated visual perception. Though, distinguishing VI from passage hallucination can be challenging since it depends on the patient's ability to determine whether there was or not a real visual external stimulation. More precise clinical criteria need to be developed in the future in order to better classify these minor manifestations and illusions. It should also be acknowledged that VI and VH are dynamic phenomena that were not occurring during the scans, even if patients had frequent and recent VI and VH at the moment of inclusion in this study. Thus, functional resting state analysis shows brain patterns at rest that could predispose to the occurrence of VI or VH in PD but does not allow to capture neural activation patterns occurring during an actual hallucinatory/illusory event.

CONCLUSION

We show both overlapping and distinct functional signatures related to VI versus VH in PD patients. This advances our current comprehension of illusions and hallucinations in PD, which have to date been limited to considering these phenomena as representing a clinical spectrum from simple to complex hallucinations. Understanding the plurality of the structural and functional characteristics underlying VI and VH in PD may enlighten how these two forms of perceptual experiences overlap and are distinct in

their specific neural dysfunction, which may inform clinical prognosis. Hence longitudinal studies focusing on structural and functional alterations in PD with VI and VH should provide greater insight into the natural history of these phenomena.

ACKNOWLEDGMENTS

This work was funded by Fondation de France (n°76354).

CONFLICT OF INTEREST

The authors have no conflict of interest to report.

SUPPLEMENTARY MATERIAL

The supplementary material is available in the electronic version of this article: https://dx.doi.org/10.3233/JPD212838.

REFERENCES

[1] Lenka A, Pagonabarraga J, Pal PK, Bejr-Kasem H, Kulisvesky J (2019) Minor hallucinations in Parkinson disease: A subtle symptom with major clinical implications. *Neurology* **93**, 259–266.

[2] Fénelon G, Mahieux F, Huon R, Ziégler M (2000) Hallucinations in Parkinson's disease: prevalence, phenomenology and risk factors. *Brain* **123(Pt 4)**, 733–745.

[3] Ffytche DH, Creese B, Politis M, Chaudhuri KR, Weintraub D, Ballard C, Aarsland D (2017) The psychosis spectrum in Parkinson disease. *Nat Rev Neurol* **13**, 81–95.

[4] Nishio Y, Yokoi K, Uchiyama M, Mamiya Y, Watanabe H, Gang M, Baba T, Takeda A, Hirayama K, Mori E (2017) Deconstructing psychosis and misperception symptoms in Parkinson's disease. *J Neurol Neurosurg Psychiatry* **88**, 722–729.

[5] Grzeczkowski L, Roinishvili M, Chkonia E, Brand A, Mast FW, Herzog MH, Shaqiri A (2018) Is the perception of illusions abnormal in schizophrenia? *Psychiatry Res* **270**, 929–939.

[6] King DJ, Hodgekins J, Chouinard PA, Chouinard V-A, Sperandio I (2017) A review of abnormalities in the perception of visual illusions in schizophrenia. *Psychon Bull Rev* **24**, 734–751.

[7] Lenka A, Jhunjhunwala KR, Saini J, Pal PK (2015) Structural and functional neuroimaging in patients with Parkinson's disease and visual hallucinations: A critical review. *Parkinsonism Relat Disord* **21**, 683–691.

[8] Goldman JG, Stebbins GT, Dinh V, Bernard B, Merkitch D, deToledo-Morrell L, Goetz CG (2014) Visuoperceptive region atrophy independent of cognitive status in patients with Parkinson's disease with hallucinations. *Brain* **137**, 849–859.

[9] Ramírez-Ruiz B, Martí M-J, Tolosa E, Giménez M, Bargalló N, Valldeoriola F, Junqué C (2007) Cerebral atrophy in Parkinson's disease patients with visual hallucinations. *Eur J Neurol* **14**, 750–756.

[10] Pagonabarraga J, Soriano-Mas C, Llebaria G, López-Solà M, Pujol J, Kulisevsky J (2014) Neural correlates of minor hallucinations in non-demented patients with Parkinson's disease. *Parkinsonism Relat Disord* **20**, 290–296.

[11] Stebbins GT, Goetz CG, Carrillo MC, Bangen KJ, Turner DA, Glover GH, Gabrieli JDE (2004) Altered cortical visual processing in PD with hallucinations: an fMRI study. *Neurology* **63**, 1409–1416.

[12] Shine JM, Muller AJ, O'Callaghan C, Hornberger M, Halliday GM, Lewis SJ (2015) Abnormal connectivity between the default mode and the visual system underlies the manifestation of visual hallucinations in Parkinson's disease: a task-based fMRI study. *NPJ Parkinsons Dis* **1**, 15003.

[13] Dujardin K, Roman D, Baille G, Pins D, Lefebvre S, Delmaire C, Defebvre L, Jardri R (2020) What can we learn from fMRI capture of visual hallucinations in Parkinson's disease? *Brain Imaging Behav* **14**, 329–335.

[14] Zmigrod L, Garrison JR, Carr J, Simons JS (2016) The neural mechanisms of hallucinations: A quantitative meta-analysis of neuroimaging studies. *Neurosci Biobehav Rev* **69**, 113–123.

[15] Ibarretxe-Bilbao N, Ramirez-Ruiz B, Junque C, Marti MJ, Valldeoriola F, Bargallo N, Juanes S, Tolosa E (2010) Differential progression of brain atrophy in Parkinson's disease with and without visual hallucinations. *J Neurol Neurosurg Psychiatry* **81**, 650–657.

[16] Ibarretxe-Bilbao N, Ramírez-Ruiz B, Tolosa E, Martí MJ, Valldeoriola F, Bargalló N, Junqué C (2008) Hippocampal head atrophy predominance in Parkinson's disease with hallucinations and with dementia. *J Neurol* **255**, 1324–1331.

[17] Meppelink AM, de Jong BM, Teune LK, van Laar T (2011) Regional cortical grey matter loss in Parkinson's disease without dementia is independent from visual hallucinations. *Mov Disord* **26**, 142–147.

[18] Holroyd S, Wooten GF (2006) Preliminary FMRI evidence of visual system dysfunction in Parkinson's disease patients with visual hallucinations. *J Neuropsychiatry Clin Neurosci* **18**, 402–404.

[19] Ramírez-Ruiz B, Martí M-J, Tolosa E, Falcón C, Bargalló N, Valldeoriola F, Junqué C (2008) Brain response to complex visual stimuli in Parkinson's patients with hallucinations: a functional magnetic resonance imaging study. *Mov Disord* **23**, 2335–2343.

[20] Yao N, Pang S, Cheung C, Chang RS-K, Lau KK, Suckling J, Yu K, Mak HK-F, McAlonan G, Ho S-L, Chua S-E (2015) Resting activity in visual and corticostriatal pathways in Parkinson's disease with hallucinations. *Parkinsonism Relat Disord* **21**, 131–137.

[21] Ishioka T, Hirayama K, Hosokai Y, Takeda A, Suzuki K, Nishio Y, Sawada Y, Takahashi S, Fukuda H, Itoyama Y, Mori E (2011) Illusory misidentifications and cortical hypometabolism in Parkinson's disease. *Mov Disord* **26**, 837–843.

[22] Marques A, Beze S, Pereira B, Chassain C, Monneyron N, Delaby L, Lambert C, Fontaine M, Derost P, Debilly B, Rieu I, Lewis SJG, Chiambaretta F, Durif F (2020) Visual hallucinations and illusions in Parkinson's disease: the role of ocular pathology. *J Neurol* **267**, 2829-2841.

[23] Nishio Y, Yokoi K, Hirayama K, Ishioka T, Hosokai Y, Gang M, Uchiyama M, Baba T, Suzuki K, Takeda A, Mori E (2018) Defining visual illusions in Parkinson's disease: Kinetopsia and object misidentification illusions. *Parkinsonism Relat Disord* **55**, 111–116.

[24] Barrell K, Bureau B, Turcano P, Phillips GD, Anderson JS, Malik A, Shprecher D, Zorn M, Zamrini E, Savica R

(2018) High-order visual processing, visual symptoms, and visual hallucinations: a possible symptomatic progression of Parkinson's disease. *Front Neurol* **9**, 999.

[25] Emberson LL, Crosswhite SL, Richards JE, Aslin RN (2017) The lateral occipital cortex is selective for object shape, not texture/color, at six months. *J Neurosci* **37**, 3698–3703.

[26] Schankin CJ, Goadsby PJ (2015) Visual snow–persistent positive visual phenomenon distinct from migraine aura. *Curr Pain Headache Rep* **19**, 23.

[27] Weiner KS, Zilles K (2016) The anatomical and functional specialization of the fusiform gyrus. *Neuropsychologia* **83**, 48–62.

[28] Zadra JR, Clore GL (2011) Emotion and perception: the role of affective information. *Wiley Interdiscip Rev Cogn Sci* **2**, 676–685.

[29] Behrendt R-P (2013) Hippocampus and consciousness. *Rev Neurosci* **24**, 239–266.

[30] Cavanna AE, Trimble MR (2006) The precuneus: a review of its functional anatomy and behavioural correlates. *Brain* **129**, 564–583.

[31] Markowitsch H (1995) Which brain regions are critically involved in the retrieval of old episodic memory? *Brain Res Rev* **21**, 117–127.

[32] Stetson C, Cui X, Montague PR, Eagleman DM (2006) Motor-sensory recalibration leads to an illusory reversal of action and sensation. *Neuron* **51**, 651–659.

[33] Simons JS, Henson RNA, Gilbert SJ, Fletcher PC (2008) Separable forms of reality monitoring supported by anterior prefrontal cortex. *J Cogn Neurosci* **20**, 447–457.

[34] Lundstrom BN, Ingvar M, Petersson KM (2005) The role of precuneus and left inferior frontal cortex during source memory episodic retrieval. *Neuroimage* **27**, 824–834.

[35] Hughes AJ, Daniel SE, Kilford L, Lees AJ (1992) Accuracy of clinical diagnosis of idiopathic Parkinson's disease: a clinico-pathological study of 100 cases. *J Neurol Neurosurg Psychiatr* **55**, 181–184.

[36] Visser M, Verbaan D, van Rooden SM, Stiggelbout AM, Marinus J, van Hilten JJ (2007) Assessment of psychiatric complications in Parkinson's disease: The SCOPA-PC. *Mov Disord* **22**, 2221–2228.

[37] Fernandez HH, Aarsland D, Fénelon G, Friedman JH, Marsh L, Tröster AI, Poewe W, Rascol O, Sampaio C, Stebbins GT, Goetz CG (2008) Scales to assess psychosis in Parkinson's disease: Critique and recommendations. *Mov Disord* **23**, 484–500.

[38] Nasreddine ZS, Phillips NA, Bédirian V, Charbonneau S, Whitehead V, Collin I, Cummings JL, Chertkow H (2005) The Montreal Cognitive Assessment, MoCA: a brief screening tool for mild cognitive impairment. *J Am Geriatr Soc* **53**, 695–699.

[39] de Chazeron I, Pereira B, Chereau-Boudet I, Brousse G, Misdrahi D, Fénelon G, Tronche A, Schwan R, Lançon C, Marques A, Debilly B, Durif F, Llorca P (2015) Validation of a Psycho-Sensory hAllucinations Scale (PSAS) in schizophrenia and Parkinson's disease. *Schizophr Res* **161**, 269–76.

[40] Movement Disorder Society Task Force on Rating Scales for Parkinson's Disease (2003) The Unified Parkinson's Disease Rating Scale (UPDRS): status and recommendations. *Mov Disord* **18**, 738–750.

[41] Hoehn MM, Yahr MD (1967) Parkinsonism: onset, progression and mortality. *Neurology* **17**, 427–442.

[42] Tomlinson CL, Stowe R, Patel S, Rick C, Gray R, Clarke CE (2010) Systematic review of levodopa dose equivalency reporting in Parkinson's disease. *Mov Disord* **25**, 2649–2653.

[43] Mattis (1988) *Dementia Rating Scale Professional Manual*. Odessa, FL.

[44] Shin M-S, Park S-Y, Park S-R, Seol S-H, Kwon JS (2006) Clinical and empirical applications of the Rey-Osterrieth Complex Figure Test. *Nat Protoc* **1**, 892–899.

[45] Chaudhuri KR, Pal S, DiMarco A, Whately-Smith C, Bridgman K, Mathew R, Pezzela FR, Forbes A, Högl B, Trenkwalder C (2002) The Parkinson's disease sleep scale: a new instrument for assessing sleep and nocturnal disability in Parkinson's disease. *J Neurol Neurosurg Psychiatr* **73**, 629–635.

[46] Postuma RB, Arnulf I, Hogl B, Iranzo A, Miyamoto T, Dauvilliers Y, Oertel W, Ju Y-E, Puligheddu M, Jennum P, Pelletier A, Wolfson C, Leu-Semenescu S, Frauscher B, Miyamoto M, Cochen De Cock V, Unger MM, Stiasny-Kolster K, Fantini ML, Montplaisir JY (2012) A single-question screen for rapid eye movement sleep behavior disorder: a multicenter validation study. *Mov Disord* **27**, 913–916.

[47] Johns MW (1991) A new method for measuring daytime sleepiness: the Epworth sleepiness scale. *Sleep* **14**, 540–545.

[48] Keenan KE, Ainslie M, Barker AJ, Boss MA, Cecil KM, Charles C, Chenevert TL, Clarke L, Evelhoch JL, Finn P, Gembris D, Gunter JL, Hill DLG, Jack CR, Jackson EF, Liu G, Russek SE, Sharma SD, Steckner M, Stupic KF, Trzasko JD, Yuan C, Zheng J (2018) Quantitative magnetic resonance imaging phantoms: A review and the need for a system phantom. *Magn Reson Med* **79**, 48–61.

[49] Whitfield-Gabrieli S, Nieto-Castanon A (2012) *Conn*: A functional connectivity toolbox for correlated and anticorrelated brain networks. *Brain Connect* **2**, 125–141.

[50] Gama RL, Bruin VMS, Távora DGF, Duran FLS, Bittencourt L, Tufik S (2014) Structural brain abnormalities in patients with Parkinson's disease with visual hallucinations: A comparative voxel-based analysis. *Brain Cogn* **87**, 97–103.

[51] Shin S, Lee JE, Hong JY, Sunwoo M-K, Sohn YH, Lee PH (2012) Neuroanatomical substrates of visual hallucinations in patients with non-demented Parkinson's disease. *J Neurol Neurosurg Psychiatry* **83**, 1155–1161.

[52] Watanabe H, Senda J, Kato S, Ito M, Atsuta N, Hara K, Tsuboi T, Katsuno M, Nakamura T, Hirayama M, Adachi H, Naganawa S, Sobue G (2013) Cortical and subcortical brain atrophy in Parkinson's disease with visual hallucination: VBM IN PD-VH. *Mov Disord* **28**, 1732–1736.

[53] Blankstein U, Chen JYW, Mincic AM, McGrath PA, Davis KD (2009) The complex minds of teenagers: neuroanatomy of personality differs between sexes. *Neuropsychologia* **47**, 599–603.

[54] Voets NL, Hough MG, Douaud G, Matthews PM, James A, Winmill L, Webster P, Smith S (2008) Evidence for abnormalities of cortical development in adolescent-onset schizophrenia. *Neuroimage* **43**, 665–675.

[55] Burghaus L, Eggers C, Timmermann L, Fink GR, Diederich NJ (2012) Hallucinations in neurodegenerative diseases. *CNS Neurosci Ther* **18**, 149–159.

[56] Meppelink AM, de Jong BM, Renken R, Leenders KL, Cornelissen FW, van Laar T (2009) Impaired visual processing preceding image recognition in Parkinson's disease patients with visual hallucinations. *Brain* **132**, 2980–2993.

[57] Yao N, Cheung C, Pang S, Shek-kwan Chang R, Lau KK, Suckling J, Yu K, Ka-Fung Mak H, Chua SE, Ho S-L, McAlonan GM (2016) Multimodal MRI of the

hippocampus in Parkinson's disease with visual hallucinations. *Brain Struct Funct* **221**, 287–300.

[58] Hamann S (2001) Cognitive and neural mechanisms of emotional memory. *Trends Cogn Sci* **5**, 394–400.

[59] Wright CI, Martis B, Schwartz CE, Shin LM, Fischer H H, McMullin K, Rauch SL (2003) Novelty responses and differential effects of order in the amygdala, substantia innominata, and inferior temporal cortex. *Neuroimage* **18**, 660–669.

[60] Greenberg DL, Rice HJ, Cooper JJ, Cabeza R, Rubin DC, Labar KS (2005) Co-activation of the amygdala, hippocampus and inferior frontal gyrus during autobiographical memory retrieval. *Neuropsychologia* **43**, 659–674.

[61] Menon V, Uddin LQ (2010) Saliency, switching, attention and control: a network model of insula function. *Brain Struct Funct* **214**, 655–667.

[62] Vogt BA (2019) Cingulate cortex in Parkinson's disease. *Handb Clin Neurol* **166**, 253–266.

[63] Lefebvre S, Baille G, Jardri R, Plomhause L, Szaffarczyk S, Defebvre L, Thomas P, Delmaire C, Pins D, Dujardin K (2016) Hallucinations and conscious access to visual inputs in Parkinson's disease. *Sci Rep* **6**, 36284.

[64] Weissman DH (2004) Dorsal anterior cingulate cortex resolves conflict from distracting stimuli by boosting attention toward relevant events. *Cereb Cortex* **15**, 229–237.

[65] Leech R, Sharp DJ (2014) The role of the posterior cingulate cortex in cognition and disease. *Brain* **137**, 12–32.

[66] Palejwala AH, O'Connor KP, Pelargos P, Briggs RG, Milton CK, Conner AK, Milligan TM, O'Donoghue DL, Glenn CA, Sughrue ME (2020) Anatomy and white matter connections of the lateral occipital cortex. *Surg Radiol Anat* **42**, 315–328.

[67] Malach R, Reppas JB, Benson RR, Kwong KK, Jiang H, Kennedy WA, Ledden PJ, Brady TJ, Rosen BR, Tootell RB (1995) Object-related activity revealed by functional magnetic resonance imaging in human occipital cortex. *Proc Natl Acad Sci U S A* **92**, 8135–8139.

[68] Kazui H, Ishii R, Yoshida T, Ikezawa K, Takaya M, Tokunaga H, Tanaka T, Takeda M (2009) Neuroimaging studies in patients with Charles Bonnet Syndrome. *Psychogeriatrics* **9**, 77–84.

[69] Vinogradov S, Luks TL, Schulman BJ, Simpson GV (2008) Deficit in a neural correlate of reality monitoring in schizophrenia patients. *Cereb Cortex* **18**, 2532–2539.

[70] Fénelon G, Alves G (2010) Epidemiology of psychosis in Parkinson's disease. *J Neurol Sci* **289**, 12–17.

[71] Llorca P, Pereira B, Jardri R, Chereau-Boudet I, Brousse G, Misdrahi D, Fénelon G, Tronche A, Schwan R, Lançon C, Marques A, Ulla M, Derost P, Debilly B, Durif F, de Chazeron I (2016) Hallucinations in schizophrenia and Parkinson"s disease: an analysis of sensory modalities involved and the repercussion on patients. *Sci Rep* **6**, 38152.

[72] Papapetropoulos S, Katzen H, Schrag A, Singer C, Scanlon BK, Nation D, Guevara A, Levin B (2008) A questionnaire-based (UM-PDHQ) study of hallucinations in Parkinson's disease. *BMC Neurol* **8**, 21.

[73] Goetz CG, Stebbins GT, Ouyang B (2011) Visual plus non-visual hallucinations in Parkinson's disease: development and evolution over 10 years. *Mov Disord* **26**, 2196–2200.

[74] Solla P, Masala C, Pinna I, Ercoli T, Loy F, Orofino G, Fadda L, Defazio G (2021) Frequency and determinants of olfactory hallucinations in Parkinson's disease patients. *Brain Sci* **11**, 841.

[75] Bannier S, Berdagué J, Rieu I, de Chazeron I, Marques A, Derost P, Ulla M, Llorca P, Durif F (2012) Prevalence and phenomenology of olfactory hallucinations in Parkinson's disease. *J Neurol Neurosurg Psychiatry* **83**, 1019–21.

[76] Kim NY, Hsu J, Talmasov D, Joutsa J, Soussand L, Wu O, Rost NS, Morenas-Rodríguez E, Martí-Fàbregas J, Pascual-Leone A, Corlett PR, Fox MD (2021) Lesions causing hallucinations localize to one common brain network. *Mol Psychiatry* **26**, 1299–1309.